^{13}C NMR Chemical Shielding Tensor of the Bridging Methylene Unit in *cis*-$(\mu\text{-}CH_2)(\mu\text{-}CO)[FeCp(CO)]_2$‡

Ae Ja Kim, Maria I. Altbach, and Leslie G. Butler*,†

Contribution from the Department of Chemistry, Louisiana State University, Baton Rouge, Louisiana 70803-1804. *Received November 14, 1990*

Abstract: The principal elements of the ^{13}C NMR chemical shielding tensor have been determined for the bridging methylene unit in *cis*-$(\mu\text{-}CH_2)(\mu\text{-}CO)[FeCp(CO)]_2$ from a combination of a Herzfeld-Berger analysis of the CP/MAS spectrum and a nonlinear least-squares fit of the proton-decoupled ^{13}C powder pattern. The $^{13}CH_2$ unit is both spatially isolated from other magnetic nuclei in the solid and largely motionally decoupled from dipolar interactions with the Cp ring protons. For the purpose of interpreting the proton-coupled ^{13}C powder pattern, we have assumed that the carbon site of the dimetallocyclopropane unit lies on the intersection of two perpendicular mirror planes of symmetry. With this assumption, there are six possible relative orientations of the $^{13}CH_2$ unit with respect to the principal axis system of the ^{13}C chemical shielding tensor; simulations of the proton-coupled ^{13}C powder patterns have been compared to the experimental spectrum, and the orientation of the chemical shielding tensor with respect to the molecular frameworks has been assigned. The C-H bond length and the H-C-H bond angle were obtained from the dipolar coupling tensor. A single, very large paramagnetic chemical shielding tensor element is a result of relatively weak carbon-metal bonds through two carbon atomic p orbitals and strong C-H bonds with the remaining carbon p orbital. Thus, these results are consistent with a molecular orbital analysis in which the methylene unit has σ-donating a_1 and π-accepting b_1 valence orbitals.

Introduction

The chemical and physical properties of bridging methylene metal dimers are fascinating.[1] With a hydride acceptor, $(\mu\text{-}CH_2)(\mu\text{-}CO)[FeCp(CO)]_2$ can be converted to a bridging methine metal cation;[2] treatment with a noncoordinating acid yields an agostic methyl-bridged cation.[3] Such reaction chemistry should be influenced in part by the charge resident on the bridging methylene carbon.[4] Two measures of carbon charge have yielded differing results. The binding energies of the C_{1s} orbital for several bridging methylene metal dimers are significantly less than for cyclopropane, indicative of a negative charge relative to the aliphatic reference.[5] Yet, for *cis*-$(\mu\text{-}C^2H_2)(\mu\text{-}CO)[FeCp(CO)]_2$, solid-state deuterium NMR shows that the electric field gradient at deuterons bound to carbon is nearly the same as found for deuterium bound to an aliphatic carbon site, suggesting the same charge as the reference.[6] The wide range of chemical and physical properties relative to an aliphatic methylene site emphasizes the importance of the metal-carbon interaction. A molecular orbital picture of the bonding between a CH_2 unit and the metal dimer has been developed by a number of groups.[7] The salient features are carbon-based σ-donating a_1 and π-accepting b_1 valence orbitals interacting with metal-based orbitals. With the presence of low-lying metal-carbon antibonding orbitals, one can anticipate an unusual ^{13}C NMR chemical shielding interaction. Herein, we report the results of a solid-state ^{13}C NMR study of a bridging methylene metal dimer, *cis*-$(\mu\text{-}^{13}CH_2)(\mu\text{-}CO)[FeCp(CO)]_2$.

An important feature of NMR studies is the ability of the spectroscopist to predict the general features of the spectrum on the basis of a knowledge of the interaction Hamiltonians, molecular geometry, molecular dynamics, and electronic structure. Because one aspect of these results is so clearly defined, the major orientation of the chemical shielding tensor, this study provides a textbook example for what is often considered an obtuse area of NMR spectroscopy, the prediction of chemical shielding interactions based upon molecular and electronic structure.

With respect to the spectroscopy, there are two features of note in this work. First, in the context of I_2S spin systems, this study is one of the few in which orientation of the ^{13}C chemical shielding tensor[8,9] has been determined with use of a powder sample[10] rather than a single crystal, though rather more examples now exist for ^{15}N.[11-14] Several techniques have been developed for dealing with powdered samples: separated local field,[15-17] analyses of critical frequencies,[13,18] dipolar modulation,[19,20] and matching a dipolar coupled powder pattern.[18,21-23] In this work, calculated proton-coupled ^{13}C powder patterns were matched to the experimental spectrum. As a check, a separated local field spectrum was also calculated and matched to the corresponding experimental

* To whom correspondence should be addressed.
† Fellow of the Alfred P. Sloan Foundation (1989-1991).
‡ Keyword index: solid-state ^{13}C NMR, bridging methylene, nanoscopic MRI, chemical shielding, dipolar coupling.

(1) Herrmann, W. A. *Adv. Organomet. Chem.* **1982**, *20*, 159-263.
(2) Casey, C. P.; Gable, K. P.; Roddick, D. M. *Organometallics* **1990**, *9*, 221-6.
(3) Casey, C. P.; Fagan, P. J.; Miles, W. H. *J. Am. Chem. Soc.* **1982**, *104*, 1134-6.
(4) (a) Bursten, B. E.; Cayton, R. H. *J. Am. Chem. Soc.* **1987**, *109*, 6053-9. (b) Bursten, B. E.; Cayton, R. H. *Polyhedron* **1988**, *7*, 943-54.
(5) Xiang, S. F.; Chen, H. W.; Eyermann, C. J.; Jolly, W. L.; Smit, S. P.; Theopold, K. H.; Bergman, R. G.; Herrmann, W. A.; Pettit, R. *Organometallics* **1982**, *1*, 1200-3.
(6) Altbach, M. I.; Hiyama, Y.; Gerson, D. J.; Butler, L. G. *J. Am. Chem. Soc.* **1987**, *109*, 5529-31.
(7) (a) Hofmann, P. *Angew. Chem., Int. Ed. Engl.* **1979**, *18*, 554-6. (b) Calabro, D. C.; Lichtenberger, D. L.; Herrmann, W. A. *J. Am. Chem. Soc.* **1981**, *103*, 6852-5. (c) Bursten, B. E.; Cayton, R. H. *J. Am. Chem. Soc.* **1986**, *108*, 8241-9.
(8) Veeman, W. S. *Prog. Nucl. Magn. Reson. Spectrosc.* **1984**, *16*, 193-235.
(9) Duncan, T. M. *J. Phys. Chem. Ref. Data* **1987**, *16*, 125-51.
(10) Mass, W. E. J. R.; Ketgens, A. P. M.; Veeman, W. S. *J. Chem. Phys.* **1987**, *87*, 6854-8.
(11) Herzfeld, J.; Roberts, J. E.; Griffin, R. G. *J. Chem. Phys.* **1987**, *86*, 597-602.
(12) Hartzell, C. J.; Pratum, T. K.; Drobny, G. *J. Chem. Phys.* **1987**, *87*, 4324-31.
(13) Teng, Q.; Cross, T. A. *J. Magn. Reson.* **1989**, *85*, 439-47.
(14) Hiyama, Y.; Niu, C.-H.; Silverton, J. V.; Bavoso, A.; Torchia, D. A. *J. Am. Chem. Soc.* **1988**, *110*, 2378-83.
(15) (a) Opella, S. J.; Waugh, J. S. *J. Chem. Phys.* **1977**, *66*, 4919-24. (b) Rybaczewski, E. F.; Neff, B. L.; Waugh, J. S.; Sherfinski, J. S. *J. Chem. Phys.* **1977**, *67*, 1231-6.
(16) Linder, M.; Höhener, A.; Ernst, R. R. *J. Chem. Phys.* **1980**, *73*, 4959-70.
(17) Duijvestijn, M. J.; Manenschijn, A.; Smidt, J.; Wind, R. A. *J. Magn. Reson.* **1985**, *64*, 461-9.
(18) Chu, P. J.; Gerstein, B. C. *J. Chem. Phys.* **1989**, *91*, 2081-101.
(19) Munowitz, M.; Huang, T.-H.; Griffin, R. G. *J. Chem. Phys.* **1987**, *86*, 4362-8.
(20) Stoll, M. E.; Vega, A. J.; Vaughan, R. W. *J. Chem. Phys.* **1976**, *65*, 4093-8.
(21) Zilm, K. W.; Beeler, A. J.; Grant, D. M.; Michl, J.; Chou, T.-C.; Allred, E. L. *J. Am. Chem. Soc.* **1981**, *103*, 2119-20.
(22) Alderman, D. W.; Solum, M. S.; Grant, D. M. *J. Chem. Phys.* **1986**, *84*, 3717-25.
(23) (a) Oas, T. G.; Drobny, G. P.; Dahlquist, F. W. *J. Magn. Reson.* **1988**, *78*, 408-24. (b) Hyde, J. S.; Pasenkiewicz-Gierula, M.; Basosi, R.; Froncisz, W.; Antholine, W. E. *J. Magn. Reson.* **1989**, *82*, 63-75.

0002-7863/91/1513-4831$02.50/0

Chart I

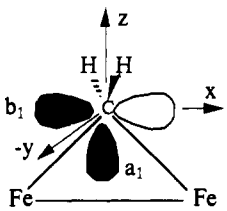

I

spectrum. Second, the ^{13}C chemical shift anisotropy for the bridging methylene site is very large, much larger than a typical methylene site[24] and exceeded only by sites such as metal carbonyls and carbon monoxide.[25,26] In fact, it is this very large chemical shift anisotropy that makes possible a qualitative correlation between the orientation of the chemical shielding tensor and the electronic structure of the bridging methylene unit.

Theory

Electronic Structure and the Chemical Shielding Tensor. Chemical shielding is a sum of paramagnetic and diamagnetic contributions: $\sigma_{\alpha\alpha} = \sigma_{\alpha\alpha}^{para} + \sigma_{\alpha\alpha}^{dia}$ ($\alpha = x, y, z$). Herein we use ^{13}C chemical shifts referenced to TMS with positive shifts to higher frequency; i.e., the isotropic chemical shift of benzene is 128.7 ppm. Therefore, $\sigma_{\alpha\alpha}^{para}$ is positive and $\sigma_{\alpha\alpha}^{dia}$ is generally negative. For ^{13}C sites in diamagnetic compounds, the diamagnetic contribution has a limiting value of about −90 ppm[26] and has less orientational dependence than the paramagnetic contribution.[27,28] Thus, we assume that most of the chemical shielding anisotropy will be due to the paramagnetic term; the component along the x-axis is given here:

$$\sigma_{xx}^{para}(\mathrm{TMS}) = \frac{\mu_0 e^2}{8\pi m} \sum_{k \neq 0} \frac{1}{(E_k - E_0)} \left[\langle \psi_0 | \sum_i L_{ix} | \psi_k \rangle \left\langle \psi_k \left| \sum_i \frac{L_{ix}}{r_i^3} \right| \psi_0 \right\rangle + \left\langle \psi_0 \left| \sum_i \frac{L_{ix}}{r_i^3} \right| \psi_k \right\rangle \langle \psi_k | \sum_i L_{ix} | \psi_0 \rangle \right] \quad (1)$$

where μ_0 is the permittivity of free space, e is the charge of the electron, and m is the mass of the electron.[29] The wave functions ψ_0 and ψ_k refer to ground and excited molecular states as do, respectively, the state energies, E_0 and E_k. With the origin at carbon, r_i is the distance to the ith electron and L_{ix} is the angular momentum operator for the ith electron. In spite of the complexity of eq 1, many useful results have been obtained by evaluating eq 1 with use of wave functions derived from molecular orbital calculations.[30-32]

Generally, there is not sufficient information to evaluate the integrals contained in eq 1. For this reason, a set of approximations is commonly applied for a simple chemical shielding analysis. These approximations are the following:

(1) The ground- and excited-state molecular wave functions can be approximated by high-lying bonding and low-lying antibonding orbitals, ϕ and ϕ^*, respectively.

(2) For integrals of the type $\langle \phi | \sum_i L_{ix} | \phi^* \rangle$, the only nonzero component is centered on the carbon site[33] and is of the form $\langle p_z | \sum_i L_{ix} | p_y \rangle \neq 0$, where the Levi-Civita angular momentum rules[34] can be used to evaluate the integral.

(3) All of the nonzero integrals have the same constant, positive value. With these quite gross, but common, approximations, the expression for the paramagnetic contribution is greatly simplified. A further simplification occurs for sites with C_{2v} symmetry; a coordinate system can be defined such that atomic p_x, p_y, and p_z orbitals at a site do not mix. Chart I shows the coordinate system for a bridging methylene site. For the carbon site, the paramagnetic contribution to the chemical shielding along the y-axis is

$$\sigma_{yy}^{para}(\mathrm{TMS}) \propto \frac{1}{(E_{a_1^*} - E_{b_1})} + \frac{1}{(E_{b_1^*} - E_{a_1})} \quad (2)$$

where E_{a_1} and $E_{a_1^*}$ are the energies of high-lying bonding and low-lying antibonding orbitals with a contribution from the carbon p_z orbital. Similarly, E_{b_1} and $E_{b_1^*}$ are related to the carbon p_x orbital. We note that expressions similar to eq 2 have been generated before.[35,36] However, the present work is unique in that the experimental data for the bridging methylene unit contains one element that is so exceedingly large that we may reasonably expect the approximations listed above to be qualitatively valid. Finally, the convention used herein for the relative assignment of the principal components of the chemical shielding tensor is $\sigma_{11} \geq \sigma_{22} \geq \sigma_{33}$ and $\sigma_{iso} = {}^1/_3(\sigma_{11} + \sigma_{22} + \sigma_{33})$; again, tensor elements, $\sigma_{\alpha\alpha}$, are referenced to TMS.[9,37]

Spectroscopy of I_2S Spin Systems. Herein, we give a brief outline of the procedure used to simulate the proton-coupled ^{13}C powder patterns. Briefly, we treat the methylene unit as an isolated three-spin system and calculate the transitions in the frequency domain by solving the time-independent total Hamiltonian for the spin-state energies.[15b,34] Carbon transition frequencies are summed over a range of possible orientations of the methylene unit with the applied magnetic field. The total Hamiltonian, in frequency units (rad s^{-1}), for the three-spin system is

$$H_{total} = H_{CS}^{C} + H_{Zeeman}^{H} + H_{dipolar}^{hetero} + H_{dipolar}^{homo} \quad (3)$$

where the chemical shielding interaction, H_{CS}^{C}, is given by

$$H_{CS}^{C} = -\hbar\gamma^{C}\mathbf{B}_0 \cdot (\tilde{1} - \tilde{\sigma}) \cdot \mathbf{S}^{C} \quad (4)$$

and where γ^C is the gyromagnetic ratio for ^{13}C, $\mathbf{B}_0$ is the applied magnetic field, $\tilde{1}$ is the identity matrix, and $\mathbf{S}^C$ is the carbon spin angular momentum operator.[34] The chemical shielding tensor, $\tilde{\sigma}$, is a second-rank tensor with nine elements. Only the symmetric components of the tensor contribute in first order to the normal NMR spectrum.[37] With the TMS scale, there is a change in sign in eq 4, such that

$$H_{CS}^{C} = -\hbar\gamma^{C} B_z^{0} (1 + \sigma_{lab}^{zz}) S_z^{C} \quad (5)$$

where we also note that the only nonzero component of the magnetic field is along the laboratory z axis. The transformation between the laboratory coordinate system (lab) and the molecular coordinate system (PA) is done with direction cosine matrices[38] by using the y-convention:[39]

$$\tilde{\sigma}_{lab} = \mathbf{R}_N^{-1}(\theta)\mathbf{R}_z^{-1}(\chi)\tilde{\sigma}_{PA}\mathbf{R}_z(\chi)\mathbf{R}_N(\theta) \quad (6)$$

The proton Zeeman interaction, H_{Zeeman}^{H}, is given by

$$H_{Zeeman}^{H} = -\hbar\gamma^{H}\mathbf{B}_z^{0}[I_{z1} + (1 + \epsilon)I_{z2}] \quad (7)$$

where I_{z1} and I_{z2} are spin angular momentum operators for hy-

(24) VanderHart, D. L. *J. Chem. Phys.* **1976**, *64*, 830-4.
(25) Gleeson, J. W.; Vaughan, R. W. *J. Chem. Phys.* **1983**, *78*, 5384-92.
(26) Beeler, A. J.; Orendt, A. M.; Grant, D. M.; Cutts, P. W.; Michl, J.; Zilm, K. W.; Downing, J. W.; Facelli, J. C.; Schindler, M. S.; Kutzelnigg, W. *J. Am. Chem. Soc.* **1984**, *106*, 7672-6.
(27) Ando, I.; Webb, G. A. *Theory of NMR Parameters*; Academic Press: New York, 1983.
(28) Dykstra, C. E. *Ab Initio Calculation of the Structures and Properties of Molecules*; Elsevier: New York, 1988.
(29) Derived from ref 27, eq 3.14.
(30) Facelli, J. C.; Grant, D. M.; Michl, J. *Acc. Chem. Res.* **1987**, *20*, 152-8.
(31) Jameson, C. J.; De Dios, A.; Jameson, A. K. *Chem. Phys. Lett.* **1990**, *167*, 575-82.
(32) (a) Nakatsuji, H.; Nakao, T.; Kanda, K. *Chem. Phys.* **1987**, *118*, 25-32. (b) Nakatsuji, H.; Nakao, T. *Chem. Phys. Lett.* **1990**, *167*, 571-4. (c) Nakatsuji, H.; Sugimoto, M. *Inorg. Chem.* **1990**, *29*, 1221-5.
(33) Pople, J. A. *Mol. Phys.* **1964**, *7*, 301-6.
(34) Gerstein, B. C.; Dybowski, C. R. *Transient Techniques in NMR of Solids*; Academic Press: New York, 1985.
(35) Karplus, M.; Pople, J. A. *J. Chem. Phys.* **1963**, *38*, 2803-7.
(36) (a) Chisholm, M. H.; Godleski, S. *Prog. Inorg. Chem.* **1976**, *20*, 299-436. (b) Jameson, C. J.; Mason, J. In *Multinuclear NMR*; Mason, J., Ed.; Plenum: New York, 1987; Chapter 3 and references therein.
(37) Haeberlen, U. *High Resolution NMR in Solids*; Academic Press: New York, 1976.
(38) Ditchfield, R.; Ellis, P. D. In *Topics in Carbon-13 NMR Spectroscopy*; Levy, G. C., Ed.; John Wiley & Sons: New York, 1974; Vol. I, pp 1-51.
(39) Zare, R. N. *Angular Momentum*; Wiley-Interscience: New York, 1988.
(40) Goldstein, H. *Classical Mechanics*, 2nd ed.; Addison-Wesley: New York, 1980. Note error in eq B-3y.

drogen at sites 1 and 2, respectively. The slight difference in chemical shift between sites 1 and 2, $\epsilon = 10^{-9}$ ppm, is made so as to render the two sets of proton spin-state energies nondegenerate as the algorithm used to assign spin quantum numbers to each proton spin state is suitable only for nondegenerate energy levels.

The dipolar interactions are separated into heteronuclear and homonuclear interactions. The heteronuclear dipolar coupling is given by

$$H_{\text{dipolar}}^{\text{hetero}} = \frac{\gamma^{C}\gamma^{H}\hbar}{|r_{\text{lab}}^{H1}|^3}\{[S_xI_{x1} + S_yI_{y1} + S_zI_{z1}] + [S_xI_{x2} + S_yI_{y2} + S_zI_{z2}]\} - 3\frac{\gamma^{C}\gamma^{H}\hbar}{|r_{\text{lab}}^{H1}|^5}\{[S_xr_{x1} + S_yr_{y1} + S_zr_{z1}][I_{x1}r_{x1} + I_{y1}r_{y1} + I_{z1}r_{z1}] + [S_xr_{x2} + S_yr_{y2} + S_zr_{z2}][I_{x2}r_{x2} + I_{y2}r_{y2} + I_{z2}r_{z2}]\} \quad (8)$$

in a molecular axis framework in which the carbon site is the origin and the vectors r_{PA}^{H1} and r_{PA}^{H2} define the positions of hydrogen sites H1 and H2, respectively, in the principal axis system. We have assumed that both C–H bond lengths are the same; $|r_{PA}^{H1}| = |r_{PA}^{H2}|$. Transformation of the vectors from the principal axis system into the laboratory axis system is again done with direction cosine matrices:

$$r_{\text{lab}}^{H1} = r_{PA}^{H1}\mathbf{R}_z(\chi)\mathbf{R}_N(\theta) \quad (9)$$

Similarly, the homonuclear dipolar coupling is given by

$$H_{\text{dipolar}}^{\text{homo}} = \frac{\gamma_H\gamma_H\hbar}{|r_{\text{lab}}^{H1} - r_{\text{lab}}^{H2}|^3}[I_{x1}I_{x2} + I_{y1}I_{y2} + I_{z1}I_{z2}] - 3\frac{\gamma_H\gamma_H\hbar}{|r_{\text{lab}}^{H1} - r_{\text{lab}}^{H2}|^5}\{[I_{x1}(r_{x1} - r_{x2}) + I_{y1}(r_{y1} - r_{y2}) + I_{z1}(r_{z1} - r_{z2})][I_{x2}(r_{x1} - r_{x2}) + I_{y2}(r_{y1} - r_{y2}) + I_{z2}(r_{z1} - r_{z2})]\} \quad (10)$$

The spin angular momentum operators are defined for the uncoupled product basis set of |H1 H2 ^{13}C⟩ by direct product expansion from the Pauli spin matrices. There are six allowed ^{13}C transitions: $|\alpha,\alpha,\alpha\rangle \rightarrow |\alpha,\alpha,\beta\rangle$, $|\alpha,\beta,\alpha\rangle \rightarrow |\alpha,\beta,\beta\rangle$, $|\alpha,\beta,\alpha\rangle \rightarrow |\beta,\alpha,\beta\rangle$, $|\beta,\alpha,\alpha\rangle \rightarrow |\beta,\alpha,\beta\rangle$, $|\beta,\alpha,\alpha\rangle \rightarrow |\alpha,\beta,\beta\rangle$, and $|\beta,\beta,\alpha\rangle \rightarrow |\beta,\beta,\beta\rangle$.[15b] The spin-state energy levels are assigned the spin quantum number of the carbon on the basis of a conditional test of the diagonal elements of $U^{\dagger}I_zU$; greater than zero indicates β and less than zero indicates α, and likewise, similar tests are performed for the two hydrogen nuclei. The unitary matrix, U, is obtained from a diagonalization of H_{total}. The carbon powder pattern, with proton dipolar coupling, is then obtained by summing the carbon transition frequencies over a range of χ,θ orientations over the range of 0–90°, inclusive, with sin θ weighting.[22] Typically, we use a uniform step angle of 2°, and the calculation takes ca. 70 min on a VAXstation 3200. Figure 1 shows the six proton coupled ^{13}C powder patterns for a methylene unit for which the axes of the dipolar and chemical shielding tensors are colinear.

Experimental Methods

The preparation of (μ-$^{13}CH_2$)(μ-CO)[FeCp(CO)]$_2$ was based on literature methods.[41] The Wittig reagent was prepared by starting from triphenylphosphine and ^{13}C-labeled (99%) methyl iodide.

$$(C_6H_5)_3P + {}^{13}CH_3I + NaH \rightarrow (C_6H_5)_3P{=}{}^{13}CH_2 + H_2 + NaI$$

$$(C_6H_5)_3P{=}{}^{13}CH_2 + (\mu\text{-CO})_2[FeCp(CO)]_2 \rightarrow cis,trans\text{-}(\mu\text{-}{}^{13}CH_2)(\mu\text{-CO})[FeCp(CO)]_2$$

Low-temperature column chromatography was used to isolate the cis isomer. cis–trans isomerization is facile in hexane solution at room temperature.[42] Also, the cis isomer can crystallize in both monoclinic[41a] and triclinic space groups.[43] On the basis of X-ray powder diffraction, both forms are present in the sample used herein. Because the structure factors for the monoclinic form are not available, the relative abundance of each form can not be calculated. However, the diffractions corresponding to the triclinic form are more intense than those due to the monoclinic form; thus, we judge that the triclinic form is more abundant.

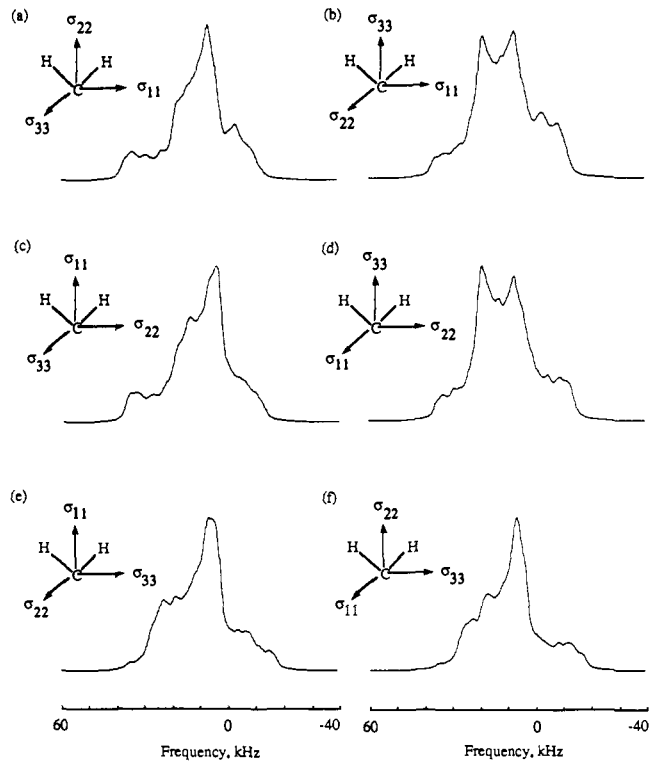

Figure 1. Calculated proton-coupled ^{13}C powder patterns for the six possible relative orientations of the chemical shielding tensor with respect to the dipolar coupling tensor for a methylene site with local C_{2v} symmetry. Important parameters in these calculations are $\sigma_{11} = 378.9$, $\sigma_{22} = 67.5$, $\sigma_{33} = -29.4$ ppm (TMS), d(C–H) = 1.1 Å, ∠H–C–H = 109.5°, $\nu(^{13}C) = 50.301$ MHz, and Lorentzian line broadening 3 kHz.

Solid-state ^{13}C NMR spectra were taken with a Bruker MSL 200 solid-state NMR spectrometer operating at 50.301 MHz for ^{13}C provided with a temperature control unit that uses a copper–constantan thermocouple junction located near the MAS stator. While there are clear advantages to performing NMR experiments and the corresponding simulations at different magnetic field strengths, this was not done here.[18,23] A 15-kHz CP/MAS probe was used and the ~80-mg powdered sample was loosely packed into a 4-mm ZrO_2 rotor with a Kel-F cap. The data acquisition was via a standard single contact Hartmann–Hahn cross-polarization pulse sequence for the sample spinning experiments.[44] Slight modifications of this pulse sequence were used for acquiring the powder patterns: The proton-decoupled ^{13}C chemical shift powder pattern was acquired as a spin-echo following an 80-μs delay. The proton-coupled ^{13}C powder pattern was also acquired as a spin-echo following an 80-μs delay; however, the proton decoupling rf irradiation was terminated at the maximum of the spin-echo. The slow spinning speed CP/MAS spectra were acquired in the same manner as the proton-decoupled ^{13}C chemical shift powder pattern; however, the delay in the spin-echo sequence was set to the inverse of the spinning rate. The proton 90° pulse was 3–5 μs, though the probe tended to arc at the higher power levels. The cross-polarization contact time ranged between 0.1 and 5 ms, and the recycle delay was 3 s. Typically, 10 000–20 000 free induction decays were acquired, and an exponential line-broadening factor of 50 Hz was applied. The chemical shielding values are recorded on the δ scale indirectly referenced through adamantane (external) to tetramethylsilane (TMS). Fourier-transformed and manually phased spectra were transferred as binary data files from the Bruker Aspect-3000 computer to a Macintosh II computer via an RS-232 serial connection and the KERMIT file transfer protocol.[45] Conversion from binary to

(41) (a) Korswagen, R.; Alt, R.; Speth, D.; Ziegler, M. L. *Angew. Chem., Int. Ed. Engl.* **1981**, *20*, 1049–51. (b) Altbach, M. I. Ph.D. Thesis, Louisiana State University, 1988.

(42) Altbach, M. I.; Muedas, C. A.; Korswagen, R. P.; Ziegler, M. L. *J. Organomet. Chem.* **1986**, *306*, 375–83.

(43) Altbach, M. I.; Fronczek, F. R.; Butler, L. G. *Acta Crystallogr., Sect C*, submitted for publication.

(44) Pines, A.; Gibby, M. G.; Waugh, J. S. *J. Chem. Phys.* **1973**, *59*, 569–90.

(45) (a) Kermit Distribution, Columbia University Center for Computing Activities, 612 West 115th St., New York, NY 10025. (b) Casey, P. K.; Jarrett, W. L.; Mathias, L. J. *Am. Lab.* (*Shelton, Conn.*) **1989**, *21*, March, 25–35.

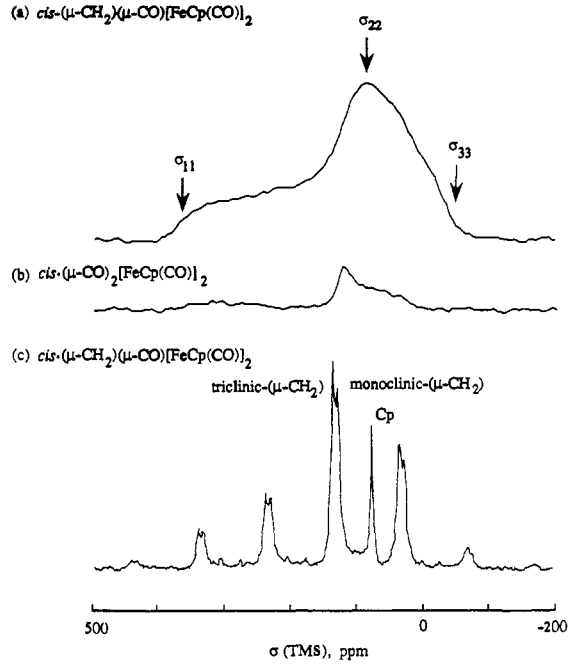

Figure 2. Solid-state NMR spectra: (a) proton-decoupled ^{13}C chemical shielding powder pattern for *cis*-(μ-$^{13}CH_2$)(μ-CO)[FeCp(CO)]$_2$, cross-polarization time of 5 ms was used at a field strength corresponding to a ^1H 90° pulse of 5 μs; (b) ^{13}C chemical shielding powder pattern for *cis*-(μ-CO)$_2$[FeCp(CO)]$_2$ showing the powder pattern for the cyclopentadienyl carbons; (c) CP/MAS spectrum of a 60:40 mixture of triclinic and monoclinic *cis*-(μ-$^{13}CH_2$)(μ-CO)[FeCp(CO)]$_2$; ν_R = 4.98 kHz, solid-state isotropic chemical shifts for the bridging methylene carbon are 145.6 and 139.0 ppm (TMS) for the triclinic and monoclinic forms, respectively, other resonances are at 87.8 ppm for the cyclopentadienyl carbons and 284.4 and 212.5 ppm for the bridging and terminal carbonyls, respectively.

ASCII data files was done with a program[46] written in LabVIEW, a graphical programming language.[47] Spectral simulation programs were written in Matlab v3.5f, a vector oriented programming language.[48] The Levenberg–Marquardt nonlinear least-square algorithm[49] was recorded in Matlab, and the data variance was assigned on the basis of a selected region of the base line. Recently developed techniques in critical frequency analysis were considered but not used.[13,18,23]

Results

The large chemical shielding anisotropy of the bridging methylene site in *cis*-(μ-$^{13}CH_2$)(μ-CO)[FeCp(CO)]$_2$ is readily apparent from the ^{13}C chemical shielding powder pattern shown in Figure 2a. The unusually large anisotropy for the methylene site is much larger than for the aromatic carbons in the cyclopentadienyl ligands of the related complex *cis*-(μ-CO)$_2$[FeCp(CO)]$_2$ shown in Figure 2b, with $\sigma_\perp$ = 122.6 (6) and $\sigma_\parallel$ = 18.2 (12) ppm (TMS).[50] The presence of two magnetically inequivalent bridging methylene sites is revealed in the CP/MAS spectrum shown in Figure 2c. The CP/MAS spectrum at 10 kHz shows two bridging methylene sites in a 60:40 relative abundance based upon peak heights, σ_{iso} = 145.6 (60% abundant, triclinic) and σ_{iso} = 139 ppm (40%, monoclinic), and where the crystal morphology is tentatively assigned on the basis of the relative intensities of the X-ray powder diffraction lines. Because of the similarity in the spinning sideband pattern, the elements of the chemical shielding tensors for both the monoclinic and triclinic sites are similar.

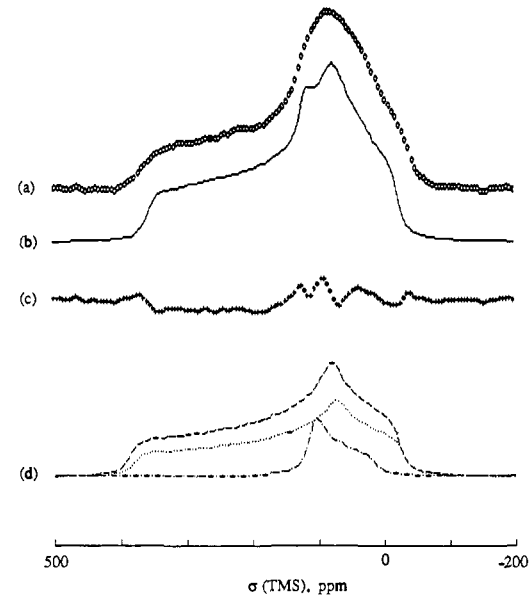

Figure 3. Results from a nonlinear least-squares analysis of the proton-decoupled ^{13}C chemical shielding powder pattern of a 60:40 mixture of triclinic and monoclinic *cis*-(μ-$^{13}CH_2$)(μ-CO)[FeCp(CO)]$_2$: (a) experimental ^{13}C chemical shielding powder pattern; (b) best calculated fit, with 1 kHz of Lorentzian line broadening, to the experimental spectrum and the corresponding residuals (c). The fit is composed of three components as shown in (d). The three components of the fit are the methylene carbons of the monoclinic form (···), the triclinic form (- - -), and the cyclopentadienyl carbons (—). The deviation at about 380 ppm may be due to finite pulse length effects.

There are several steps in the determination of the elements of the chemical shielding tensor and its orientation with respect to the molecular axis system. First, the proton-decoupled ^{13}C powder pattern was fitted to a model consisting of monoclinic and triclinic bridging methylene sites plus a contribution from the Cp carbons. Second, a Herzfeld–Berger analysis was done to verify an assumption made in the previous model. Third, the proton-coupled ^{13}C powder pattern was compared to the calculated patterns shown in Figure 1. Fourth, the fit to the proton-coupled ^{13}C powder pattern was optimized by varying d(C–H) and ∠H–C–H. Fifth, the assigned orientation was confirmed by the correspondence between experimental and calculated 2D separated local field spectra.

Figure 3 shows the results of a nonlinear least-squares fit to the chemical shielding powder pattern. The fitted variables include σ_{11}^{mono} and σ_{22}^{mono}; the value of σ_{33}^{mono} is determined from σ_{11}^{mono} and σ_{22}^{mono} and the isotropic chemical shift. We make the assumption that $\sigma_{\alpha\alpha}^{tri} = \sigma_{\alpha\alpha}^{mono} + 6.6$ ppm (α = 1, 2, 3); the reason for this constraint is the close correspondence between the two chemical shielding tensors that would otherwise lead to a singularity in the nonlinear least-squares fitting. Finally, a fixed contribution from the Cp carbons sites is also included. With this model, we find σ_{11}^{mono} = 365.7 (6), σ_{22}^{mono} = 75.5 (1), and σ_{33}^{mono} = 24.2 (6) ppm. The value of χ_ν^2 = 2.0 (step angle 2°, data variance 2%) indicates that this model is tenable. There are two sources of systematic errors that are of concern: anisotropic cross-polarization and finite pulse length effects. Briefly, anisotropic cross-polarization is evident as a decreased cross-polarization rate at orientations ("magic angle") for which the dipolar coupling between ^1H and ^{13}C is quenched.[24,51] An interesting experiment to test for anisotropic cross-polarization in this system would be to acquire the ^{13}C chemical shielding powder pattern without cross-polarization and compare the fit of this data to the model. Unfortunately, the long ^{13}C T_1, on the order of 100 s, precluded

(46) Michaels, D. C.; Kim, A. J.; Perilloux, B. C.; Barksdale, D.; Butler, L. G. *Comput. Chem.*, submitted for publication.
(47) LabVIEW, National Instruments Corp., 6504 Bridge Point Parkway, Austin, TX 78730.
(48) Matlab, The Mathworks Inc., 24 Prime Parkway, Natick, MA 01760.
(49) (a) Bevington, P. R. *Data Reduction and Error Analysis for the Physical Sciences*; McGraw-Hill: New York, 1969. (b) Press, W. H.; Flannery, B. P.; Teukolsky, S. A.; Vetterling, W. T. *Numerical Recipes*; Cambridge University Press: Cambridge, 1986.
(50) Result of the best nonlinear least-squares fit of the spectrum shown in Figure 2b.
(51) (a) Griffin, R. G. *Methods Enzymol.* **1981**, *72*, 108–74. (b) Levitt, M. H.; Suter, D.; Ernst, R. R. *J. Chem. Phys.* **1986**, *84*, 4243–55.

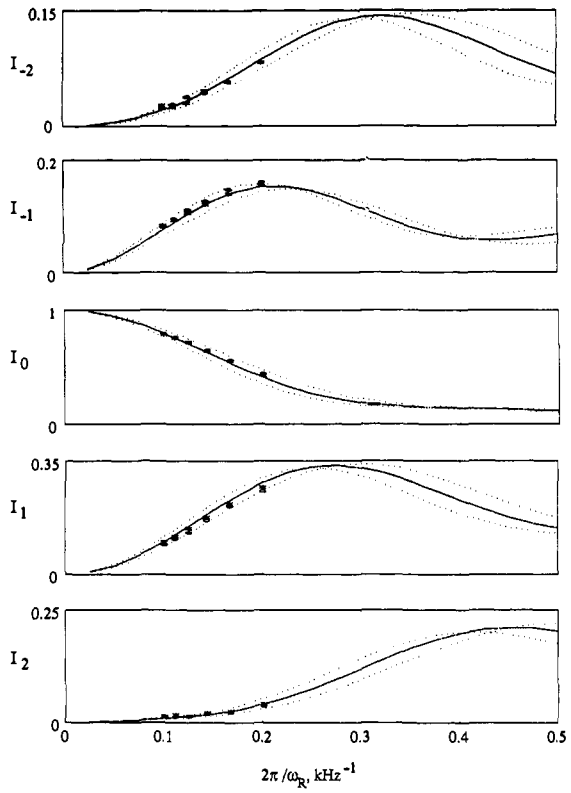

Figure 4. Traces show the calculated intensities of a central band and related spinning sidebands based on a Herzfeld–Berger analysis of the CP/MAS experiment. The solid traces are based on the monoclinic form with σ_{11} = 365.7, σ_{22} = 75.5, and σ_{33} = −24.2 ppm. The experimental central and sideband intensities of the monoclinic form are indicated as with an asterisk. The data for the triclinic form are shown as a circle by making the assumption that $\sigma_{\alpha\alpha}^{tri} = \sigma_{\alpha\alpha}^{mono} + 6.6$ ppm (α = 1, 2, 3). The dotted lines are to indicate the precision of this experiment and are shown for ±20 ppm variations in $\sigma_{33} - \sigma_{22}$ and $\sigma_{iso} - \sigma_{11}$. Spin rates range from 5 to 10 kHz; below 5 kHz, there was interference from the Cp ring spinning sideband pattern.

acquisition of the spectrum without cross-polarization. Finite pulse length effects would be evident as a reduced intensity in the experimental spectrum at the extremes. We note that the fit is poorest at 20 kHz, as would be expected for a systematic error due to finite pulse length effects.

In a Herzfeld–Berger analysis, the relative intensities of the spinning sidebands in series of CP/MAS spectra are used to determine the elements of the chemical shielding tensor.[52] However, here we have used the Herzfeld–Berger analysis for a more restricted application, verifying the difference between the chemical shielding tensor elements of the monoclinic and triclinic sites. Shown in Figure 4 are the results of the analysis, which show that $\sigma_{\alpha\alpha}^{tri} = \sigma_{\alpha\alpha}^{mono} + 6.6$ ppm (α = 1, 2, 3). It is possible to show the results for both sites since the calculated spinning sideband intensities depend only on the values of $\sigma_{33} - \sigma_{22}$ and $\sigma_{iso} - \sigma_{11}$. Because the experimental spinning sideband intensities for both crystallographic forms can be fitted to the same set of calculated traces, the constant 6.6 ppm difference between tensor elements of the two forms is confirmed. We note, however, that this technique is not particularly sensitive at the spin rates we can access.

Figure 5a shows the proton-coupled ^{13}C powder pattern for *cis*-(μ-$^{13}CH_2$)(μ-CO)[FeCp(CO)]$_2$. A simple comparison of the experimental results with the previously calculated spectra suggests a match with chemical shielding orientation shown in Figure 1a. The match with one of the spectra of Figure 1 indicates that the methylene unit can be treated as an isolated $^{13}CH_2$ spin system. Also, the Cp rings are rapidly rotating about an axis from the iron atom through the centroid of the Cp ring. In the related

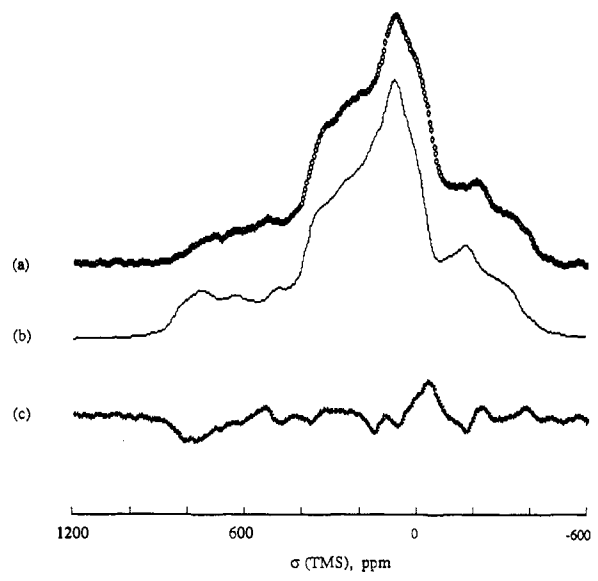

Figure 5. Results from a nonlinear least-squares analysis of the proton-coupled ^{13}C powder pattern of *cis*-(μ-$^{13}CH_2$)(μ-CO)[FeCp(CO)]$_2$ with the orientation shown in Figure 1a: (a) experimental proton-coupled ^{13}C powder pattern, cross-polarization time of 5 ms was used at a field strength corresponding to a ^1H 90° pulse of 5 μs; (b) best calculated fit, with 3 kHz of Lorenztian line broadening, to the experimental spectrum, χ_ν^2 = 2.7 with a step angle of 2°, fit is composed of two components, the methylene carbons of the monoclinic and triclinic forms; (c) residual, negative deviation at about 800 ppm may be due to finite pulse length effects.

complex *cis*-(μ-CO)$_2$[FeCp(CO)]$_2$, the Cp rings are executing C_5 jumps at a rate of (2.4 (5)) × 10^{11} s^{-1}.[53] With this rapid motion, the dipolar interaction between the $^{13}CH_2$ unit and the protons of the Cp rings is much reduced. The jump rate is temperature dependent. Since spectra taken at −10 and +40 °C showed no significant variations, aside from random noise, from the spectrum shown in Figure 5a, we conclude that dipolar coupling between the $^{13}CH_2$ unit and the Cp protons is negligible.

The result of the nonlinear least-squares fit to the proton-coupled ^{13}C powder pattern is shown in Figure 5b where the fitted variables are vertical scale and vertical offset. Fixed parameters include the isotropic chemical shifts for the triclinic and monoclinic forms, the 60:40 relative abundance, d(C–H) = 1.1 Å, and ∠H–C–H = 109.5°. The contribution of the Cp ring sites to the proton-coupled ^{13}C powder pattern was ignored since the spectrum of *cis*-(μ-CO)$_2$[FeCp(CO)]$_2$ showed only a weak, broad resonance. The value of χ_ν^2 is 2.7 (step angle 2°, data variance 2%), indicating that the model is tenable. Again, there is a possibility that systematic error may have been caused by anisotropic cross-polarization. We note here the similarity in the pulse sequences used to acquire the spectra in Figures 4a and 5a. Since we have shown in Figure 4a that a ^{13}C spin-echo has been prepared without detectable flaw caused by anisotropic cross-polarization, we can then expect the proton-coupled ^{13}C powder pattern to be similarly unafflicted by artifacts. Thus, we are assured that apparent good fit of the proton-coupled ^{13}C powder pattern to Figure 1a is not an accidental coincidence associated with a powder pattern modulated by anisotropic cross-polarization.

A proton-coupled powder pattern contains geometric information. We recall that the fit shown in Figure 5b was obtained with a fixed methylene geometry. The proton-coupled ^{13}C powder pattern was fitted while allowing the parameters d(C–H) and ∠H–C–H to vary. The nonlinear least-squares routine successfully converged on the values d(C–H) = 1.122 (3) Å and ∠H–C–H = 110.8 (4)°, and the value of χ_ν^2 is reduced to 2.1; thus, the fit is significantly better at the 95% confidence level than for the previous fit with fixed d(C–H) and ∠H–C–H. For the comparison

(52) Herzfeld, J.; Berger, A. E. *J. Chem. Phys.* **1980**, *73*, 6021–30.

(53) Altbach, M. I.; Hiyama, Y.; Wittebort, R. J.; Butler, L. G. *Inorg. Chem.* **1990**, *29*, 741–7.

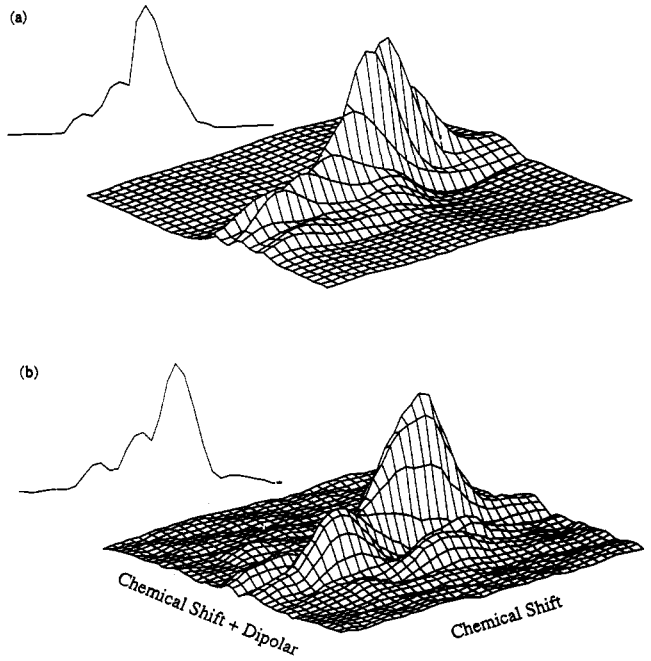

Figure 6. Calculated (a) and experimental (b) 2D separated local field spectra of *cis*-(μ-$^{13}CH_2$)(μ-CO)[FeCp(CO)]$_2$. The pulse sequence of Linder et al. was used with a 5-μs 90° ^{1}H pulse and evolution with 141 kHz off resonance decoupling.[16] Also shown are the calculated and experimental dipolar projections along the F1 dimension. The calculated results are obtained with the same chemical shielding tensor elements and orientation as used for the 1D simulation in Figure 5.

of bond lengths determined from NMR dipolar couplings with those obtained from scattering experiments such as neutron diffraction, compensation must be made for the effect of molecular motions upon the measurements.[54] For the NMR experiments, Henry and Szabo have shown that the averaging of $\langle 1/r^3 \rangle$ for a ^{13}C–H unit is affected by the C–H stretching vibration and the librational motions of the molecule.[55] Generally, vibrational averaging of the NMR dipolar coupling acts to weaken the interaction such that the uncorrected bond length is too long, about 2.3% (propane methylene)[55] to 2.7% (benzene).[56] If extensive librational motions are present, say for the methylene units in solid octane, even larger correction factors are required.[55] On the basis of the C–H stretching frequency for the bridging methylene site,[6] and if we also assume that libration motions are similar to those for the propane methylene, then the corrected value of d(C–H) is 1.096 (3) Å. For comparison, the bridging methylene geometries in related rhodium and osmium complexes as determined from neutron diffraction are as follows: *trans*-(μ-CH_2)[RhCp(CO)]$_2$, d(C–H) = 1.095 (2), 1.094 (2) Å and ∠H–C–H = 110.4 (1)°;[57] (μ-H)$_2$(μ-CH_2)$Os_3(CO)_{10}$, d(C–H) = 1.090 (11), 1.091 (10) Å and ∠H–C–H = 106.0 (8)°.[58] In the X-ray crystallography work for *cis*-(μ-CH_2)(μ-CO)[FeCp(CO)]$_2$, the methylene hydrogen atoms were located and refined isotropically to give d(C–H) = 0.95 (3) and 1.00 (4) Å and ∠H–C–H = 110 (3)°.[43] The correspondence between the corrected NMR distance and those obtained from neutron diffraction is exceptionally good. But given the uncertainty associated with the librational motions, the correspondence may be coincidental.

A 2D separated local field spectrum was acquired and is shown in Figure 6. The general features of the 2D spectrum correspond well with the calculated 2D spectrum obtained with the orientation of the chemical shielding as shown in Figure 1a. The dipolar projection along the F1 dimension is particularly sensitive to the orientation of the chemical shielding tensor, and the experimental and calculated projections agree quite well. The 2D results confirm the orientation previously assigned on the basis of the 1D results.

Discussion

The chemical shielding elements for *cis*-(μ-$^{13}CH_2$)(μ-CO)-[FeCp(CO)]$_2$ cover a very large range relative to methylene units in organic compounds; for comparison, in *n*-eicosane, CH_3CH_2-($^{13}CH_2$)$_{16}CH_2CH_3$, the chemical shielding elements (TMS scale) are σ_{11} = 50.2 (20), σ_{22} = 38.2 (20), and σ_{33} = 17.2 (20).[24] The chemical shielding elements are comparable to those found for CO and for terminally bound metal carbonyls: ^{13}CO (20 K, argon matrix), σ_{11} = 305, σ_{22} = 305, and σ_{33} = −48;[26] (μ-^{13}CO)$_2$-[FeCp(CO)]$_2$, σ_{11} = 354, σ_{22} = 354, and σ_{33} = −85.[25]

It is often difficult to correlate chemical shielding in organometallic complexes with chemical bonding. One approach that appears particularly useful requires either Xα[59] or Fenske–Hall calculations of model complexes; Fenske and co-workers successfully modeled the ^{13}C chemical shift of metal carbenes and alkyls[60] and ^{11}B chemical shifts in metalloboranes.[61] However, due to three factors, we have an extremely fortunate situation here in which to apply a simplified chemical shielding analysis: large chemical shielding anisotropy, local C_{2v} symmetry for the dimetallacyclopropane unit, and published results of molecular orbital calculations. These three factors facilitate a correlation between chemical shielding and chemical bonding. The correlation requires two main components. First, the paramagnetic contribution to the chemical shielding elements is related to the energies of the bonding and antibonding orbitals and the appropriate angular momentum operators as was done in eq 2 for the chemical shielding tensor element directed along the y-axis. Second, a molecular orbital diagram for a dimetallacyclopropane unit is prepared on the basis of the best available information.

In a parameter-free Fenske–Hall calculation of (μ-CH_2)(μ-CO)[FeCp(CO)]$_2$, Bursten and Cayton determined the energies of molecular bonding and antibonding orbitals derived from the a_1 and b_1 frontier orbitals of the methylene unit; the relative energies of three out of the four orbitals are given in Figure 2 of their paper: $a_1 \leftrightarrow b_1$ = 3.2 eV and $a_1 \leftrightarrow b_1^*$ = 9.2 eV.[4a] The other necessary orbital energies are a_1 = −14.47, a_1^* = −2.27, b_2(C–H) = −26.15, b_2^*(C–H) = 53.25 eV; only the highest occupied and lowest lying virtual orbital energies are given here.[62] We note here the reported tendency for Fenske–Hall calculations to spread the energy levels of ligand orbitals.[63] That feature is not important here as only orbital energy ordering and approximate spacings are required for the qualitative analysis of the chemical shielding tensor.

In Figure 7, the energies of molecular orbitals with significant methylene carbon atomic p orbital contribution are shown. The energies for cyclopropene are taken from the results of an SCF-HF calculation with a double-ζ basis set.[64] The energies for the dimetallacyclopropane unit are taken from the work of Bursten and Cayton with the assumptions listed above. The dashed lines between the two systems illustrate the evolution of the methylene carbon atomic p orbitals between the two bonding environments. The vertical double-headed arrows indicate the nonzero angular momentum integrals that contribute to the chemical shielding, analogous to eq 2. The experimental chemical shielding elements in the indicated coordinate system for both cyclopropene[65] and

(54) See, for example: Roberts, J. E.; Harbison, G. S.; Munowitz, M. G.; Herzfeld, J.; Griffin, R. G. *J. Am. Chem. Soc.* **1987**, *109*, 4163–9.
(55) Henry, E. R.; Szabo, A. *J. Chem. Phys.* **1985**, *82*, 4753–61.
(56) Diehl, P. In *Nuclear Magnetic Resonance of Liquid Crystals*; Emsley, J. W., Ed.; D. Reidel: Boston, Chapter 7.
(57) Takusagawa, F.; Fumagalli, A.; Koetzle, T. F.; Herrmann, W. A. *Inorg. Chem.* **1981**, *20*, 3060–4.
(58) Schultz, A. J.; Williams, J. M.; Calvert, R. B.; Shapley, J. R.; Stucky, G. D. *Inorg. Chem.* **1979**, *18*, 319–23.
(59) Freier, D. G.; Fenske, R. F.; You, X.-Z. *J. Chem. Phys.* **1985**, *83*, 3526–37.
(60) Fenske, R. F. In *Organometallic Compounds*; Shapiro, B. L., Ed.; Texas A&M University Press: College Station, TX, 1983; pp 305–33.
(61) Fehlner, T. P.; Czech, P. T.; Fenske, R. F. *Inorg. Chem.* **1990**, *29*, 3103–9.
(62) Bruce E. Bursten, private communication.
(63) Bursten, B. E.; Cotton, F. A.; Stanley, G. G. *Isr. J. Chem.* **1980**, *19*, 132–42.
(64) Snyder, L. C.; Basch, H. *Molecular Wave Functions and Properties*; John Wiley & Sons: New York, 1972.
(65) Zilm, K. W.; Conlin, R. T.; Grant, D. M.; Michl, J. *J. Am. Chem. Soc.* **1980**, *102*, 6672–6.

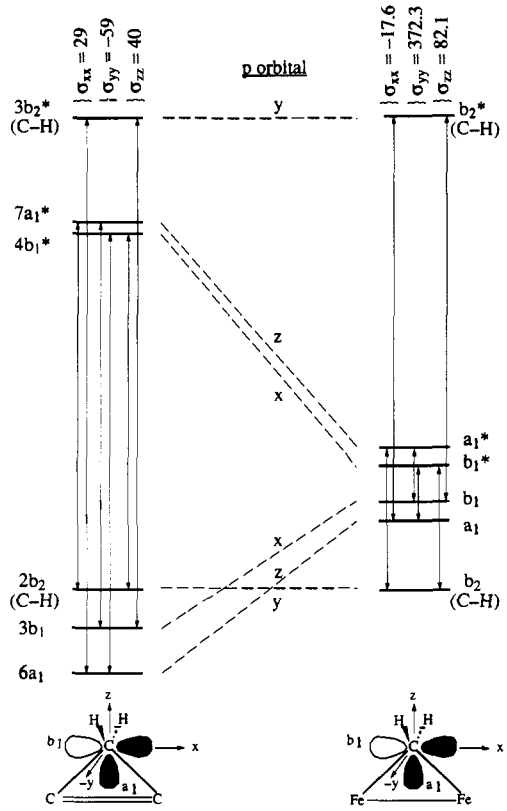

Figure 7. Molecular orbital correlation diagram for cyclopropene and a dimetallocyclopropane unit. The orbital energies for cyclopropene are from an SCF-HF calculation with a double-ζ basis set; the axis system shown for cyclopropene is the same as used in the calculation.[64] The chemical shielding tensor elements for cyclopropene are listed above the manifold.[65] The orbital energies for the dimetallacyclopropane unit are taken, in part, from the results of a Fenske–Hall calculation of *cis*-(μ-CH_2)(μ-CO)[FeCp(CO)]$_2$;[4a] the energy scale and reference for the Fenske–Hall calculation are different than those of the SCF-HF work. In particular, the energy of the C–H antibonding orbital is, as expected, anomalously high;[63] however, that is not a problem for this qualitative analysis. The chemical shielding tensor elements listed above the manifold are from this work rewritten in the coordinate system defined by cyclopropene. The dashed lines connecting orbitals of the two manifolds indicate the evolution of atomic p orbitals on the methylene carbon. The vertical double-headed arrows indicate nonzero contributions to the paramagnetic chemical shielding interaction. The length of each arrow represents the inverse of the magnitude of the contribution as detailed in eq 2.

the dimetallacyclopropane unit (this work) are given above the respective manifolds.

Cyclopropene represents the typical situation where there is no apparent qualitative correlation between the chemical shielding elements and the reciprocal of differences among the orbital energies. We conclude that there is no single element of the chemical shielding tensor that is large enough to make the gross approximations inherent in eq 2 valid.

However, for the dimetallacyclopropane unit, there is a strong qualitative correlation between the largest element of the chemical shielding tensor and the close energy spacing among molecular orbitals composed of carbon atomic p_x and p_z orbitals. There is a very large paramagnetic contribution to the chemical shielding tensor element directed along the *y*-axis as shown in Figure 7 and detailed here:

$$\sigma_{yy}^{\text{total}}\ (\text{TMS}) = \sigma_{yy}^{\text{dia}} + \sigma_{yy}^{\text{para}} = \sigma_{yy}^{\text{dia}} + k\left[\frac{1}{(a_1^* - b_1)} + \frac{1}{(b_1^* - a_1)}\right] = 372.3\ (6)\ \text{ppm} \quad (11)$$

Thus, we conclude that the frontier orbital analysis indicated in Chart I is consistent with the NMR results for the major orientation of the chemical shielding tensor.

The simplified chemical shielding analysis is clearly of limited utility. For example, the orbital energy levels of the dimetallacyclopropane unit suggest that σ_{xx} and σ_{yy} should be nearly equal. Again, it is apparent that one element of the chemical shielding tensor must be very large so that the approximations leading to eq 2 are made valid. Alternatively, there may be a significant error in the orbital energy spacings in Figure 7, most likely in the placement of a_1^* (see above).

We now turn to a brief discussion of the charge on the methylene carbon and possible inferences from the chemical shielding data. Generally, it is the diamagnetic contribution to the chemical shielding tensor that is most relevant to questions of charge.[66] In the case of axial symmetry, the paramagnetic contributions cancel for $\sigma_{\parallel}$ and a fiducial value of the diamagnetic contribution of −90 ppm was found for sp-hybridized carbon sites.[26,67] Since the methylene unit lacks axial symmetry, the most negative chemical shielding element, which is along the *x*-axis, is likely to have both paramagnetic and diamagnetic contributions. Therefore, σ_{xx}^{dia} may range anywhere from −17.6 (6) to −90 ppm to even some much more negative value, if there should be a large negative charge on the methylene carbon. Very roughly, the σ_{xx}^{dia} term should change by about −65 ppm or greater for an additional unit of negative charge.[68] A second unknown is whether there is a change in the radial distribution function of the carbon orbitals between the bridging methylene site and axial symmetric sites for which the fudical mark of $\sigma_{\parallel}$ = −90 ppm was determined. Thus, we can draw no conclusions from the chemical shielding data regarding the charge on carbon.

Conclusions

The complete orientation of the chemical shielding tensor has been obtained for a methylene unit in an organometallic complex. The determination was based upon the local symmetry of the methylene site (two orthogonal mirror planes) and the asymmetric dipolar coupling tensor due to the two methylene protons. The strength of the dipolar interaction was used to measure the methylene geometry: d(C–H) = 1.096 (3) Å (corrected for vibrational effects) and ∠H–C–H = 110.8 (4)°. The sample consisted of two crystallographic forms of *cis*-(μ-$^{13}CH_2$)(μ-CO)[FeCp(CO)]$_2$. For the triclinic form, the chemical shielding tensor elements are σ_{11} = 372.3 (6) (perpendicular to the dimetallacyclopropane ring), σ_{22} = 82.1 (1) (bisects the two hydrogens of the CH_2 unit), and σ_{33} = −17.6 (6) ppm (TMS) (parallel to the Fe–Fe bond axis). The elements of the monoclinic form are very similar: $\sigma_{\alpha\alpha}^{\text{mono}} = \sigma_{\alpha\alpha}^{\text{tri}} - 6.6$ ppm (α = 1, 2, 3).

The principal elements of the chemical shielding tensor are correlated, by using a simplified chemical shielding analysis, with the published results of a Fenske–Hall molecular orbital calculation. On the basis of the symmetry and relative energies of the bonding and antibonding orbitals, the largest paramagnetic chemical shielding tensor element is predicted to be perpendicular to the plane of the dimetallacyclopropane unit, in excellent agreement with the experimental observation. However, the limitations of the simplified chemical shielding analysis are quite obvious on two counts: First, an incorrect prediction is made for the two paramagnetic chemical shielding elements in the plane of the dimetallacyclopropane unit. Second, the diamagnetic chemical shielding elements are not determined from the simplified analysis; thus, no information is available regarding charge on the methylene carbon.

For several reasons, this study of a $^{13}CH_2$ unit provides a textbook example for a simple analysis of the paramagnetic contribution to the chemical shielding tensor. (1) Because of the C_{2v} symmetry, the otherwise complex angular momentum integrals of the chemical shielding interaction can be dealt with by using the Levi–Civita rules. (2) Because two of the carbon p orbitals participate in C–Fe bonds and one in the much stronger C–H bonds,[69] there is a conveniently large separation between sets of

(66) (a) Wu, W.-X.; You, X.-Z.; Dai, A.-B.; Jing, S.-P. *Polyhedron* **1990**, *9*, 1849–54. (b) Bodner, G. M.; Todd, L. J. *Inorg. Chem.* **1974**, *13*, 1335–8.
(67) Pople, J. A. *Proc. R. Soc. London, A* **1957**, *239*, 541–9.
(68) Malli, G.; Froese, C. *Int. J. Quantum Chem.* **1967**, *1S*, 95–8.

bonding and antibonding carbon valence orbitals. Therefore, one element of the chemical shielding tensor has a much larger paramagnetic contribution than the other two. (3) The dipolar coupling interaction allows not only the assignment of the chemical shielding tensor orientation, but also the determination of local molecular geometry ("nanoscopic MRI").

An extension of this work, NMR sensitivity permitting,[70] is the qualitative prediction and observation of surface-bound species. The detection of bridging methylene units on surfaces has been particularly difficult.[71] Given that various aspects of the problem are already known in some detail, bonding[72] and Knight shift,[73] it should be possible to qualitatively predict some aspects of the chemical shielding tensor for a surface-bound species.

Acknowledgment. The support of the National Science Foundation (Grant CHE-8715517) is gratefully acknowledged. The purchase of the Bruker MSL 200 NMR spectrometer was made possible by NSF Grant CHE-8711788. Useful discussions with R. W. Hall, N. R. Kestner, B. E. Bursten, G. G. Stanley, E. T. Samulski, D. G. Cory, and A. N. Garroway are gratefully acknowledged. L.G.B. is a Fellow of the Alfred P. Sloan Foundation (1989-1991).

Note Added in Proof. A recent compilation by Duncan[74] nicely clarifies the issue of chemical shift scales. To make our labels consistent with Duncan's, change σ to δ except for eq 4.

(69) Collman, J. P.; Hegedus, L. S.; Norton, J. R.; Finke, R. G. *Principles and Applications of Organotransition Metal Chemistry*; University Science Books: Mill Valley, CA, 1987; Table 6.1.
(70) See, for example: Pruski, M.; Kelzenberg, J. C.; Gerstein, B. C.; King, T. S. *J. Am. Chem. Soc.* **1990**, *112*, 4232-40.
(71) Albert, M. R.; Yates, J. T., Jr. *The Surface Scientist's Guide to Organometallic Chemistry*; American Chemical Society: Washington, DC, 1987.
(72) (a) Zheng, C.; Apeloig, Y.; Hoffmann, R. *J. Am. Chem. Soc.* **1988**, *110*, 749-74. (b) Hoffmann, R. *Rev. Mod. Phys.* **1988**, *60*, 601-28.
(73) (a) Wang, P.-K.; Slichter, C. P.; Sinfelt, J. H. *Phys. Rev. Lett.* **1984**, *53*, 82-5. (b) Ansermet, J.-P.; Wang, P.-K.; Slichter, C. P.; Sinfelt, J. H. *Phys. Rev. B* **1988**, *37*, 1417-28.
(74) Duncan, T. M. *A Compilation of Chemical Shift Anisotropies*; Farragut Press: Chicago, 1990.

Determination of Lateral Diffusion Coefficients in Air-Water Monolayers by Fluorescence Quenching Measurements

F. Caruso,[†] F. Grieser,[†] A. Murphy,[†] P. Thistlethwaite,*[,†] R. Urquhart,[†] M. Almgren,[‡] and E. Wistus[‡]

Contribution from the Chemistry School, Melbourne University, Parkville 3052, Australia, and Department of Physical Chemistry, University of Uppsala, S-75121 Uppsala, Sweden.
Received November 19, 1990. Revised Manuscript Received February 11, 1991

Abstract: The fluorescence quenching of a lipoidal pyrene derivative, by two amphiphilic quenchers, at the air-water interface, has been studied by steady-state and time-resolved methods. The results have been analyzed in the theoretical framework of diffusion-controlled quenching in a two-dimensional environment to yield the mutual lateral diffusion coefficients.

Introduction

The biological significance of lateral diffusion of molecules embedded in membranes has led to a number of studies of lateral diffusion in natural membranes and phospholipid bilayers[1-12] and in monolayers.[13-18] The monolayer at the air-water interface is a particularly useful model system in which to study lateral diffusion because of the control that can be exerted over the composition and packing of the monolayer, as well as the nature of the subphase. There has however been some controversy as to how well diffusion in the monolayer models that in the membrane. Early studies of diffusion in monolayers at the air-water interface, using various techniques, yielded values of the diffusion coefficient at least an order of magnitude larger than those reported earlier for lipid bilayers and membranes.[13-15]

There have been a number of approaches to the measurement of lateral diffusion coefficients in monolayers. In what might be termed the "direct" approach, the movement of a probe molecule from one region to another is monitored by some suitable technique. The diffusion coefficient is unambiguously defined in terms of the average distance diffused per unit time. An example of this approach is the fluorescence recovery after photobleaching (FRAP) technique,[1,2,13,18] which involves monitoring the regrowth of fluorescence due to fluorophores diffusing into a pulse photobleached region. While being straightforward in interpretation, the FRAP method faces experimental difficulties related to surface flow, caused by minute temperature gradients at the air-water interface. Such surface streaming can interfere with the diffusion

* To whom correspondence should be addressed.
[†] Melbourne University.
[‡] University of Uppsala.

(1) Peters, R. *Cell Biol. Int. Rep.* **1981**, *5*, 733.
(2) Cherry, R. J. *Biochim. Biophys. Acta* **1979**, *559*, 289.
(3) Edidin, E. In *Membrane Structure*; Finean, J. B., Michell, R. H., Eds.; Elsevier/North-Holland: Amsterdam, 1981.
(4) Wu, E.-S.; Jacobson, K.; Papahajopoulos, D. *Biochemistry* **1977**, *16*, 3936.
(5) Galla, H.-J.; Sackmann, E. *Ber. Bunsen-Ges. Phys. Chem.* **1974**, *78*, 949.
(6) Galla, H.-J.; Sackmann, E. *Biochim. Biophys. Acta* **1974**, *339*, 103.
(7) Kano, K.; Kawazumi, H.; Ogawa, T.; Sunamoto, J. *J. Phys. Chem.* **1981**, *85*, 2204.
(8) Trauble, H.; Sackmann, E. *J. Am. Chem. Soc.* **1972**, *94*, 4499.
(9) Devaux, P.; McConnell, H. M. *J. Am. Chem. Soc.* **1972**, *94*, 4475.
(10) Scandella, C. J.; Devaux, P.; McConnell, H. M. *Proc. Natl. Acad. Sci. U.S.A.* **1972**, *69*, 2056.
(11) Vanderkooi, J. M.; Fischkoff, S.; Andrich, M.; Podo, F.; Owen, C. S. *J. Chem. Phys.* **1975**, *63*, 3661.
(12) Miller, D. D.; Evans, D. F. *J. Phys. Chem.* **1989**, *93*, 323.
(13) Teissié, J.; Tocanne, J.-F.; Baudras, A. *Eur. J. Biochem.* **1978**, *83*, 77.
(14) Loughran, T.; Hatlee, M. D.; Patterson, L. K.; Kozak, J. *J. Chem. Phys.* **1980**, *72*, 5791.
(15) Stroeve, P.; Miller, I. *Biochim. Biophys. Acta* **1975**, *401*, 157.
(16) Subramanian, R.; Patterson, L. K. *J. Am. Chem. Soc.* **1985**, *107*, 5820.
(17) Bohorquez, M.; Patterson, L. K. *J. Phys. Chem.* **1988**, *92*, 1835.
(18) Peters, R.; Beck, K. *Proc. Natl. Acad. Sci. U.S.A.* **1983**, *80*, 7183.

0002-7863/91/1513-4838$02.50/0